Pergamon

Journal of Structural Geology, Vol. 16, No. 10, pp. 1335 to 1352, 1994

0191-8141/94 $7.00+0.00

0191-8141(94)E0009-N

Strain partitioning across a fold and thrust belt: the Rhenish Massif, Mid-European Variscides

D. DITTMAR

Institut für Geologie, Universität Würzburg, Pleicherwall 1, D-97070 Würzburg, Germany

W. MEYER

Geologisches Institut, Universität Bonn, Nussallee 8, D-53115 Bonn, Germany

O. ONCKEN

GeoForschungsZentrum Potsdam, Telegrafenberg C2, D-14473 Potsdam, Germany

TH. SCHIEVENBUSCH

Schlumberger Geoquest, Buchholzer Strasse 100, D-30635 Hannover, Germany

R. WALTER

Geologisches Institut, Rheinisch Westfälische Technische Hochschule Aachen, Wullnerstrasse 2, D-52056 Aachen, Germany

and

C. VON WINTERFELD

GeoForschungsZentrum Potsdam, Telegrafenberg C2, D-14473 Potsdam, Germany

(*Received* 15 *March* 1993; *accepted in revised form* 10 *January* 1994)

Abstract—Strain data across the entire western Rhenish Massif illustrate the pattern of deformation partitioning within a fold and thrust belt from the foreland on the northern front of the European Variscides to the suture with the internal zones of higher metamorphic grade. Shortening perpendicular to cleavage increases from 16 to 27% (constant volume assumed) in the northern Rhenish Massif to 51% at the southern border. These values correspond to a weak general layer-parallel shortening of the basin filling in cross-section on the order of about 5–15% and more in the case of volume loss. The geometry of apparent finite strain is nearly plane strain except in the Venn Anticlinorium where strain is apparent prolate and near the southern margin of the Massif where it is apparent oblate. Net orogenic shortening in the upper crust of the fold and thrust belt is approximately 42%. It is mainly achieved by folding and tectonic stacking of the deformed basin filling, which was apparently detached from the lower crust.

Distribution of strain in the orogenic wedge is controlled by different factors at different scales. Heterogeneity is caused by changes in lithology and average grain size, by the structural position of samples in folds and their distance from thrusts in the hangingwall (at deeper crustal levels), and by the regional distribution of the metamorphic grade, i.e. by the dominant deformation mechanism. This last factor causes an exponential increase of strain with approach to the ductile lower crust. The superposition of strain partitioning mechanisms on different scales creates a complex regional strain pattern. The southern part of the thrust belt apparently suffered late westward motion (in gently dipping imbricates) or strike-parallel motion (in steeply dipping imbricates) which is probably due to oblique convergence between the Rhenohercynian and Saxothuringian microplates.

INTRODUCTION

THE distribution and geometry of deformation in continental crust which has gone through a collisional orogeny has attracted the interest of structural geology for nearly a century. Studies in the central Appalachians (e.g. Cloos 1947), the Walisian slate belt (e.g. Sorby 1908, Wood 1974), the Helvetic nappe pile of the Alps (e.g. Ramsay & Huber 1983, Dietrich 1989) show that the distribution of strain is heterogeneous on all scales and that a general increase of finite strain can be observed towards the internal and originally deeper parts of an orogenic belt. Few data, however, exist on the systematic variation of deformation from the undeformed foreland of a fold and thrust belt towards the more internal zones. Also the relevant data presently

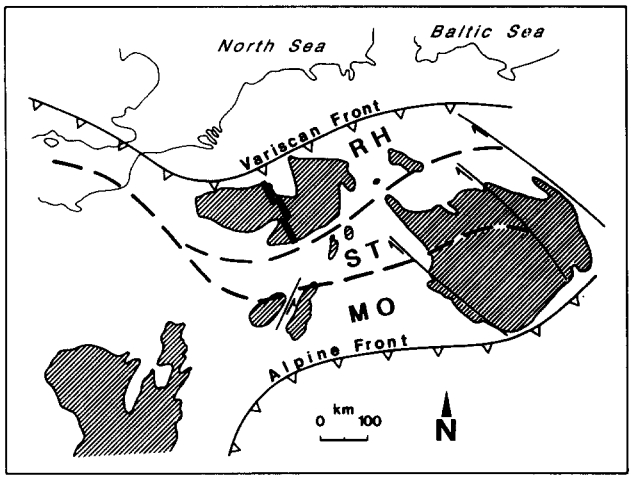

Fig. 1. Schematic map of exposed parts of the Mid-European Variscides showing the principal Variscan zones: RH, Rhenohercynian zone; ST, Saxothuringian zone; MO, Moldanubian zone and the traverse studied in this paper (outlined black areas).

mostly cover the upper crust—the geometry of orogenic deformation of the lower crust in general remains a matter of debate or indirect inference.

This study focuses on the Rhenish Massif which forms part of the Rhenohercynian fold and thrust belt on the northern flank of the Central European Variscan belt (Fig. 1). A number of reflection seismic sections have been recorded recently across this belt, revealing much new information on its deep structure (DEKORP Research Group 1985, 1991, Franke *et al.* 1990). Along one of these sections (DEKORP 1; Fig. 2) a comprehensive geological study has been carried out in order to examine the internal geometry of the belt. Its purpose is to derive a balanced paleogeographic reconstruction of the Rhenohercynian basin and to estimate the amount and local intensity of crustal contraction (Schievenbusch 1992, Dittmar 1994, von Winterfeld 1994). To accomplish this, a study was made of the distribution and geometry of the finite strain in the entire crust involved. The present paper mainly discusses the role and geometry of internal 'ductile' deformation of the thrust belt.

Earlier studies on deformation in the Rhenish Massif have been performed by Breddin (1956, 1957) and Wunderlich (1964). They found a decrease in shortening from south to north with a gross reduction of the former basin width of some 50%, but beside the general assumption of oblate strain they also lack sufficient detail for large-scale analyses.

GEOLOGICAL FRAMEWORK

Kossmat (1927) has divided the Central-European Variscan chain into several segments with different tectono-metamorphic histories (see Fig. 1). Recent interpretation regard each segment as a minor plate or terrane with Paleozoic continental basin sedimentation (Weber & Behr 1983, Matte 1986, Weber 1986, Ziegler 1986, Franke 1989), successively accreted from early Devonian times until the Late Carboniferous involving SE-directed subduction of minor intervening ocean basins. Final continental collision occured along two suture zones separating the Rhenohercynian from the Saxothuringian and the latter from the central Moldanubian zone (Fig. 1). Other, more important but largely obscured NW-dipping sutures have been assumed south of the Moldanubian zone (e.g. Frisch *et al.* 1984, Eisbacher *et al.* 1989, von Raumer & Neubauer 1993).

Within this geodynamic scenario the Rhenohercynian zone on the northern flank of the belt forms the external fold and thrust belt (lower plate). It links the undeformed foreland in the north and the suture with the Saxothuringian zone (upper plate) in the south. Crustal stretching at the beginning of the Lower Devonian led to basin formation in the western Rhenohercynian on basement constituted of lower Paleozoic sediments and medium-grade gneisses. During the Devonian and Lower Carboniferous a sedimentary pile of 3–12 km (Meyer & Stets 1980) accumulated in a passive continental margin setting. It consists of shallow-marine clastics and carbonates, intercalated in the east with abundant bimodal volcanics. The southernmost imbricates of the Rhenohercynian zone probably represent the strongly telescoped slope and rise sequences bordering a small southern oceanic basin between the Rhenohercynian and Saxothuringian Zones, indicated by MORB-type metabasalts (Meisl 1990, Dittmar & Oncken 1992). Relics of a former supracrustal nappe system in the southeastern part of the Rhenish Massif, the Giessen nappe, also contain MORB-type volcanics with Mid-Devonian cherts. These are superposed by flysch of Upper Devonian age (Engel *et al.* 1983, Grösser & Dörr 1986). The small ocean basin must be rooted between the Rhenohercynian and Saxothuringian zones, and was closed by the end of the Devonian. The subsequent northward migration of flysch sedimentation, during the Lower and Upper Carboniferous, reflects the prograding front of synmetamorphic orogenic contraction (Ahrendt *et al.* 1983, Engel & Franke 1983). Concomitant deformation at very low (in the north) to low grade conditions (in the south) resulted in the 150–200 km wide Rhenohercynian fold and thrust belt.

In response to the metamorphic conditions, deformation is controlled by flexural-slip with frictional sliding and some pressure solution in the north. The importance of pressure solution increases towards the south, and deformation becomes progressively more pervasive. At the southern margin recrystallization of quartz, calcite and mica mark the transition to the predominantly ductile regime (Oncken 1989, 1991).

The Rhenish Massif (Fig. 2) also shows several distinct changes in structural style from the northern foreland to the suture with the Saxothuringian microplate. In the north, thin-skinned deformation predominates with a major basal detachment, blind thrust splays and concentric to box-type slightly NW-vergent folds. Towards the south the thick folded and cleaved Devonian basin filling progressively forms large imbricate fans separated by prominent SE-dipping thrusts (Siegen, Boppard and Taunuskamm thrusts; Fig. 4). All

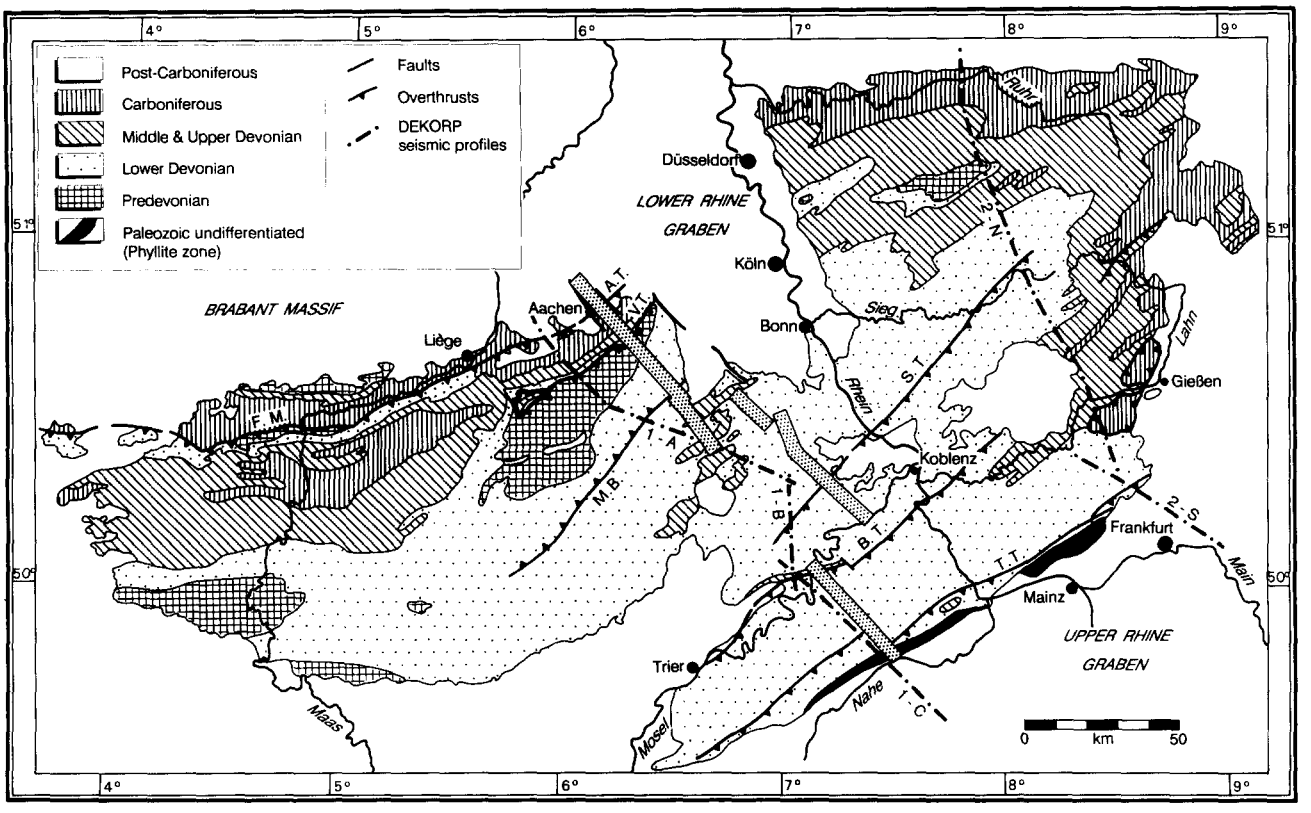

Fig. 2. Geological map of the Rhenish Massif showing DEKORP 1 and 2 seismic lines and the traverse studied in this paper (outlined stippled areas). F.M., Faille du Midi; A.T., Aachen thrust; M. B., Malsbenden backthrust; S.T.; Siegen thrust; B.T., Boppard thrust; T.T., Taunus thrust.

major thrust systems seem to be rooted in a crustal scale décollement at a depth of 13–16 km. At the southern margin of the Rhenish Massif this structural style is overprinted by backfolding which results in an overturned steeply dipping stack of high-pressure rocks with multiple folding and cleavage formation (Anderle *et al.* 1990).

Late-orogenic kinematics of the Rhenish Massif involve oblique convergence and subsequent dextral strike-slip along its southern suture during the early Upper Carboniferous (Oncken 1988, 1989, Korsch & Schäfer 1991). Upper Carboniferous and Lower Permian molasse deposits mark the onset of gravitational collapse of the thickened Variscan crust, resulting in a chain of basins aligned along the former suture (cf. Lorenz & Nicholls 1984).

STRAIN ANALYSIS

Objects

Finite strain analysis was mainly carried out on detrital grains (quartz, pebbles, ooids) in clastic sediments. Fossils (crinoid stems, corals, brachiopods) have been rarely used. Rare volcanics yield feldspar phenocrysts or filled vesicles. The detrital quartz grains are seldom recrystallized because in most parts of the Rhenish Massif synorogenic temperatures were either below the recrystallization threshold of quartz, or the grains are devoid of crystal plastic strain due to their occurrence in a matrix-supported shaly fabric which took up most strain in the shale dominated lithological sequences.

The lithologies selected for the determination of finite strain were chosen to be characteristic of the Paleozoic sedimentary sequence within each investigated region (usually ranging from sandstones and quartzites to immature shales). This procedure ensured that data points are comparable. This allows recognition of the regional strain types and unstraining of structural sections. Some 700 samples were collected, generally at distances of less than 300–400 m along the entire 150 km section (see Fig. 2). Strain heterogeneities are thus generally resolved on the map scale. Particularly interesting cases of strain heterogeneity on a smaller scale were studied through denser sampling.

Methods

Strain determination was usually performed using either the centre-to-centre-technique or Fry-analysis (Fry 1979), or applying the R_f/Φ'-method (Ramsay 1967, Dunnett 1969). The choice of the method was determined by the type of fabric and strain marker in a sample.

The Fry-method was applied in the cases of:

(1) matrix-supported detrital grains with obviously greater competence than the matrix, including evidence for pressure solution resulting in strain partitioning between matrix and marker grains; and

(2) approximately random-normal distribution of objects which were equidimensional within a 50%-limit.

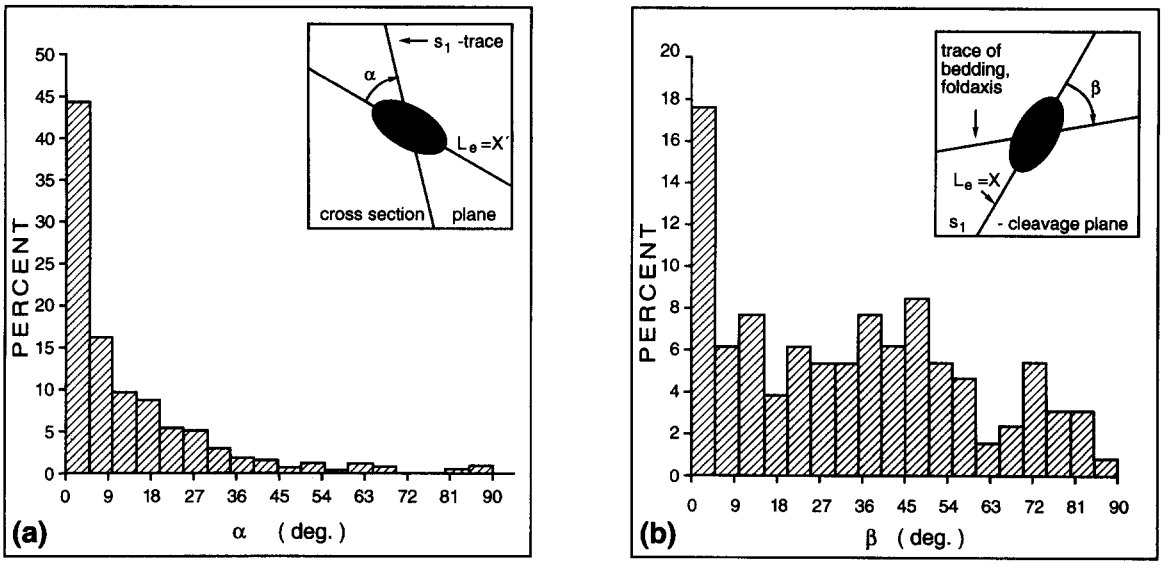

Fig. 3. Orientation of finite strain axes with reference to fabrics. (a) Deviation α of long axis of finite strain ($L_e = X'$) from trace of cleavage (s_1) in cross-section plane, *CS*-plane (280 samples evaluated). (b) Deviation β of *X*-axis of finite strain ellipsoid from axes of folds/bedding–cleavage intersection lineation (usually subhorizontal) in *XY*-plane (131 samples evaluated).

The effects of anticlustering and variable particle size were partly corrected using the method of Erslev (1988).

The R_f/Φ'-method was preferred in the cases of:

(1) grain-supported fabrics in largely monomineralic rocks with predominant deformation of markers by crystalplasticity or no more than weak cataclasis; and

(2) no more than a weak sedimentary orientation of markers (in some cases primary orientation was tested according to the method of De Paor 1988).

Analyses and calculations were performed using an automated procedure with either the software package INSTRAIN (Erslev 1988, Erslev & Ge 1990) or with an image analysis system. A minimum of 60 (R_f/Φ'-analysis) to 250 objects (Fry-analysis) was digitized from each sample using enlarged micrographs of thin sections.

All samples were cut roughly perpendicular to the trend of fold axes and cleavage planes of the dominant fabric (usually B_1, s_1), or perpendicular to the mostly subhorizontal bedding–cleavage intersection lineation. The axial ratio measured in this plane which parallels the cross-section is here termed R_{cs}. For 50% of the samples additional cuts were made parallel to the cleavage plane. The cleavage plane can be shown to approximate the *XY*-plane of the finite strain ellipsoid in slates and silty shales with a deviation of the *X*-axis from the cleavage plane well below 10–15° in well foliated rocks (see Fig. 3a). At least one set of strain data was obtained in one of the principal planes of strain. By comparison with the *XY*-plane (Fig. 3b) the cross-section-parallel cuts (R_{cs}) were often found to be oblique to the principal planes of the strain ellipsoid. The values of all principle planes of strain were calculated from these data (von Winterfeld & Oncken in preparation). Moreover, from these data shortening values are calculated with respect to different co-ordinate systems: earth co-ordinates (i.e. horizontal shortening), strain co-ordinates (i.e. principal stretches) and bedding co-ordinates (i.e. shortening of bed length).

Sources of error

Some general sources of error in the data evaluation that have to be taken into account result from inaccurate digitizing, and from graphic determination of the ellipse shape from the Fry-plot or the R_f/Φ'-curves. In the case of vaguely defined point distributions this is estimated to remain below some 10% of the true strain value. Undetected grain boundary sliding will generally lead to an underestimate of finite strain because neither shape nor centre-distances of markers are greatly affected by major rock deformation through this mechanism; however, in the generally weakly deformed rocks of the Rhenish Massif this effect is not expected to have a major impact. Asymmetrical solution of marker grains has the effect of a shifting of the grain centres and is shown to lead to an underestimate of the true strain inversely proportional to the finite strain (Dunne *et al.* 1990). In our analyses this effect becomes evident when Fry-strain computed from samples where the marker axes have been digitized is compared to results where grain centres have been digitized. In the latter case—because of the operators bias towards a 'corrected', eccentrically digitized centre at the position of the centre of a circumscribed ellipse—strain data are somewhat higher and thus closer to the true strain.

The comparison of different strain gauges or of different methods on the same markers does not give a significant difference in the results. Strain from fossils was found to be equal to Fry- or R_f/Φ'-strain to within 8% (fossil imprints or internal casts). The comparison of Fry- and R_f/Φ'-strain for the same sample shows an even more consistent relationship. The first may be higher by some 5% on average, especially where evidence of

pressure solution is obvious. The R_f/Φ'-values are normally higher in monomineralic rocks. The harmonic mean of the aspect ratio of the detrital grains, taken by many workers to be closely similar to the R_f/Φ'-values (Lisle 1977, Paterson 1983, Ramsay & Huber 1983, Ratschbacher 1987), is seen to range slightly below the R_f/Φ'-values. The difference is generally not significant. The values obtained in the present investigation by different methods seem to be compatible in this overall relatively low strain region with ellipticities in the XZ-plane ranging between 1 and 6.

RESULTS

The ellipses in Fig. 4 show the average orientation and shape of the finite strain ellipse R_{cs} of a homogeneous unit in the plane of a generalized cross-section. A homogeneous unit is defined by its coherent structural association, facies and lithology. The cross-section shows a general increase of strain from the foreland basin in the northwest to the boundary with the internal suture zone in the southeast. The strain data increase in discrete steps. Very low strains are evident in the vicinity of the foreland and in the Eifel synclinorium–depression. Axial ratios may reach 1.4, but usually are below 1.3. In many cases strain is purely compactional with uniaxial shortening perpendicular to bedding. The Venn Anticlinorium, between these two areas, shows a largely symmetrical increase of finite strain with a peak value at 1.7 on the southern flank of the anticline. Towards the southern Massif, finite strain increases in steps across the major thrusts, especially at the Boppard-Merl thrust system. The southern border of the Massif, in the Phyllite Zone, has accumulated the highest strains, reaching 2.4 on average at the southern margin. The orientation of the averaged strain ellipses in the section plane points to a progressive increase of NW–SE-shortening by internal deformation from 14 to 51% in respect to the horizontal. Detailed analysis of the strain data however exhibits considerable heterogeneity which suggests a number of relevant strain partitioning mechanisms within the orogenic wedge.

Lithology- and fold-related strain heterogeneities

Although small-scale strain heterogeneities were not of major interest in the present investigation some data were collected in order to assess the related strain variability and its causes. Lithology plays a major role: grain size distribution and composition strongly control the rheology of rocks in the case of pressure solution. Since primarily siliciclastic rocks were analysed, only grain size effects have been assessed. Samples which show graded bedding are taken to be the best gauges for evaluating heterogeneities related to effects of grain-size and variable quartz–mica ratios under otherwise constant conditions. The example shown in Fig. 5 with a span of grain sizes and mineral composition characteristic for most of the Rhenish Massif clearly illustrates the progressive change of finite strain and its orientation with continuous cleavage refraction. This is clear evidence of strain refraction due to variable viscosity ratios within the sequence, similar to the model presented by Treagus (1988). Furthermore, with increasing strain towards the more fine-grained and mica-richer layers, the deviation between the long axis of the strain ellipse and the cleavage trace in the section plane decreases to values below the accuracy of measurement. On the whole however, strain variability due to lithological reasons does not seem to exceed some 25% in the rock sequence encountered, or 0.3–0.35 units in the range of finite strains/axial ratios encountered.

Folds have long been known to show a distinct pattern of strain distribution which varies with fold type and position within the fold (Cloos 1947, Pfiffner 1980, Treagus & Treagus 1981, Ramsay & Huber 1983, Reks & Gray 1983, etc.). As with grain-size related effects, the fold-related variability of finite strain is recorded in order to assess its influence when constructing retrodeformable cross-sections. In non-metamorphic rocks, where folds of 1B- and 1C-type (Ramsay 1967) predomi-

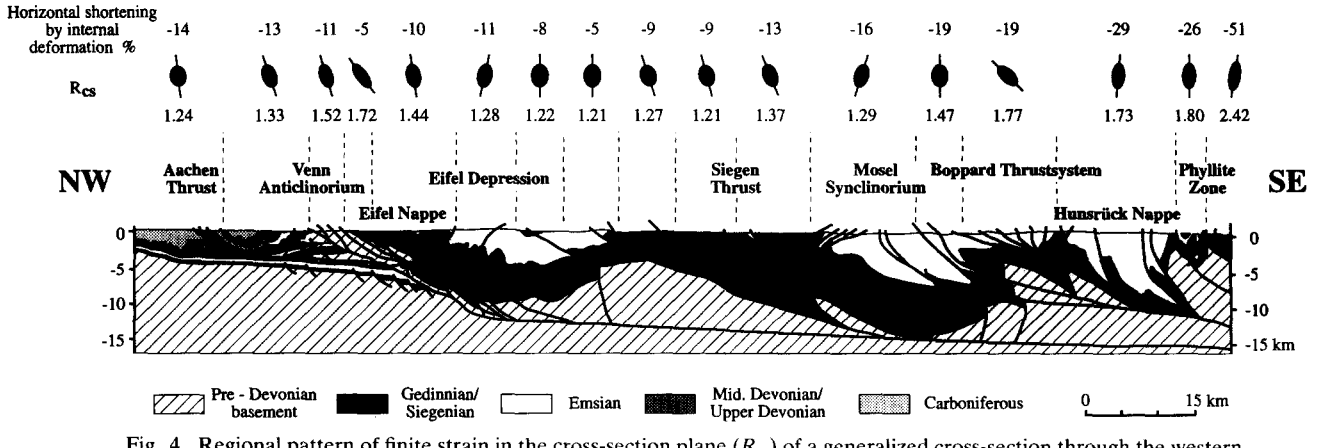

Fig. 4. Regional pattern of finite strain in the cross-section plane (R_{cs}) of a generalized cross-section through the western Rhenish Massif. For line of section see Fig. 2. Depicted ellipses show average shape and orientation of strain ellipse and the average horizontal shortening due to internal deformation for homogeneous units.

nate, strain variability within a layer of constant grain size and composition is low and may be neglected (Fig. 6a). Rocks deformed under very low–low grade conditions, with predominantly 1C-, 2- and even 3-type folds, show variations nearly twice the order of magnitude recorded from grain-size effects (<0.6–0.7 units, see Fig. 6b). The largest strain is generally observed near the hinge or on overturned limbs of very close folds, decreasing rapidly and then remaining constant with increasing distance from the hinge. The size of folds—with wavelengths between some metres to several 100 m—does not seem to have a significant influence on this pattern.

Regional fault-related strain heterogeneities

Faults record a major discontinuous partitioning of strain during deformation of the crust. Through most of the Western Rhenish Massif the distribution of finite strain has been observed to correlate strongly with the position of major thrusts and the sense of motion of the respective hangingwall.

In the northwest—at a high structural level in the fold-thrust belt—deformation occurs predominantly by flexural-slip and frictional sliding with weak bedding-internal strain. No distinct strain gradient is observed towards a major fault (Fig. 8a). Deformation is strongly localized into discrete brittle fractures, the number of which increases in the vicinity of major faults (see Wojtal 1986, for similar observations on deformation of foreland thrust sheets).

The central and southern parts of the Massif, with pervasive pressure solution and some crystal-plastic strain at a deeper level at peak paleotemperatures in the range of 200–300°C, show very different strain gradients related to two specific generations of faults. Foreland facing thrusts and backthrusts with a clear-cut cogenetic relationship to folds and dominant cleavage (mostly fault propagation folds with axial planar synmetamorphic cleavage parallel to the thrusts) constitute an early fault generation with foliated cataclasites to mylonites in the shear zones. These faults have obviously originated during peak metamorphic conditions. Some later movement during cooling and exhumation is evident from the microfabric and rank determinations which may both show the presence of a metamorphic hiatus across the thrusts (Oncken 1991). A later generation of cross-cutting, out-of-sequence thrusts with cataclastic shear zone rocks lacks the mentioned relationship and shows a strain pattern typical of the northern Massif.

Within the hanging-wall of a thrust of the first generation, strain progressively increases towards the fault over 500–1500 m subperpendicular to the faults. In an imbricate stack, the result is a strain profile which, in section view, creates a zig-zag pattern of finite strain (see Figs. 7 and 8a–c). This pattern is largely independent of folds and rock type and has proven to be a valuable tool to locate thrusts in an otherwise rather monotonous Lower Devonian clastic sequence with little internal stratigraphic resolution.

Furthermore, the shape of the strain gradient and the distribution of finite strain seem to bear a close relationship to the internal geometry of a single imbricate: internally folded imbricates and imbricates with a fault-propagation fold at the front of the body show steeper strain gradients near the thrust (<500–1000 m) down to lower finite strains within the thrust sheet (Figs. 8b–c). In comparison internally unfolded thrust bodies show a linear decrease of finite strain over a distance of more than 1500 m (cf. Fig. 8c). Overall shortening, however, remains at the same level with respect to the percentage of shortening of the basin filling.

Strain pattern and metamorphic grade

The different structural units of the Massif—each with different lithology, metamorphic grade and internal geometry—show different strains which remain rather uniform within the unit. Strain distribution is obviously controlled by the metamorphic grade of the outcropping units. The order of magnitude of paleotemperatures can be estimated from data on organic rank, from scarce mineral assemblages, and from deformation textures related to thermally activated deformation mechanisms (see Wolf 1978, Teichmüller 1979, Schievenbusch 1992, Dittmar 1994, von Winterfeld 1994, for rank data across the western Rhenish Massif, and Oncken 1991 for microfabrics). Non-metamorphic areas (peak temperatures <100°C at vitrinite reflectance < 2–3% R_{max}) are nearly devoid of internal deformation (aspect ratios <1.2 in the section plane) or only show compactional strains (nearly uniaxial shortening perpendicular to bedding). With increasing temperatures, strain increases irrespective of the distance of the sample position to the orogenic suture. At the upper range of very low grade conditions (temperatures >250°C at vitrinite reflectance > 5–6% R_{max}) aspect ratios in the XZ-plane exceed 2.0. This occurs on the southern flank of Venn Anticlinorium and in the Hunsrück Phyllite Zone. Due to the proximity to the suture the Phyllite Zone shows higher strains than the southern Venn Anticlinorium despite similar temperatures. Interestingly, although T-data are only semi-quantitative, this dependance of average finite strain on paleotemperatures reveals a nearly exponential relationship including an increasing variability towards higher temperatures (Fig. 9). The potential of high finite strains appears to increase drastically with the onset of thermally activated deformation and fabric-forming processes in quartz–phyllosilicate rocks (recovery processes and related work softening, pressure solution, grain nucleation and growth, etc.).

Geometry and orientation of finite strain

In an earlier paper, Breddin (1956) assumed that the Rhenish Massif slates generally show an oblate flattening geometry which, according to Wood (1974), is a frequent observation in slate belts. The present analysis, however, is at variance with this inference. The geometry of the strain ellipsoids varies considerably—$dV = 0$

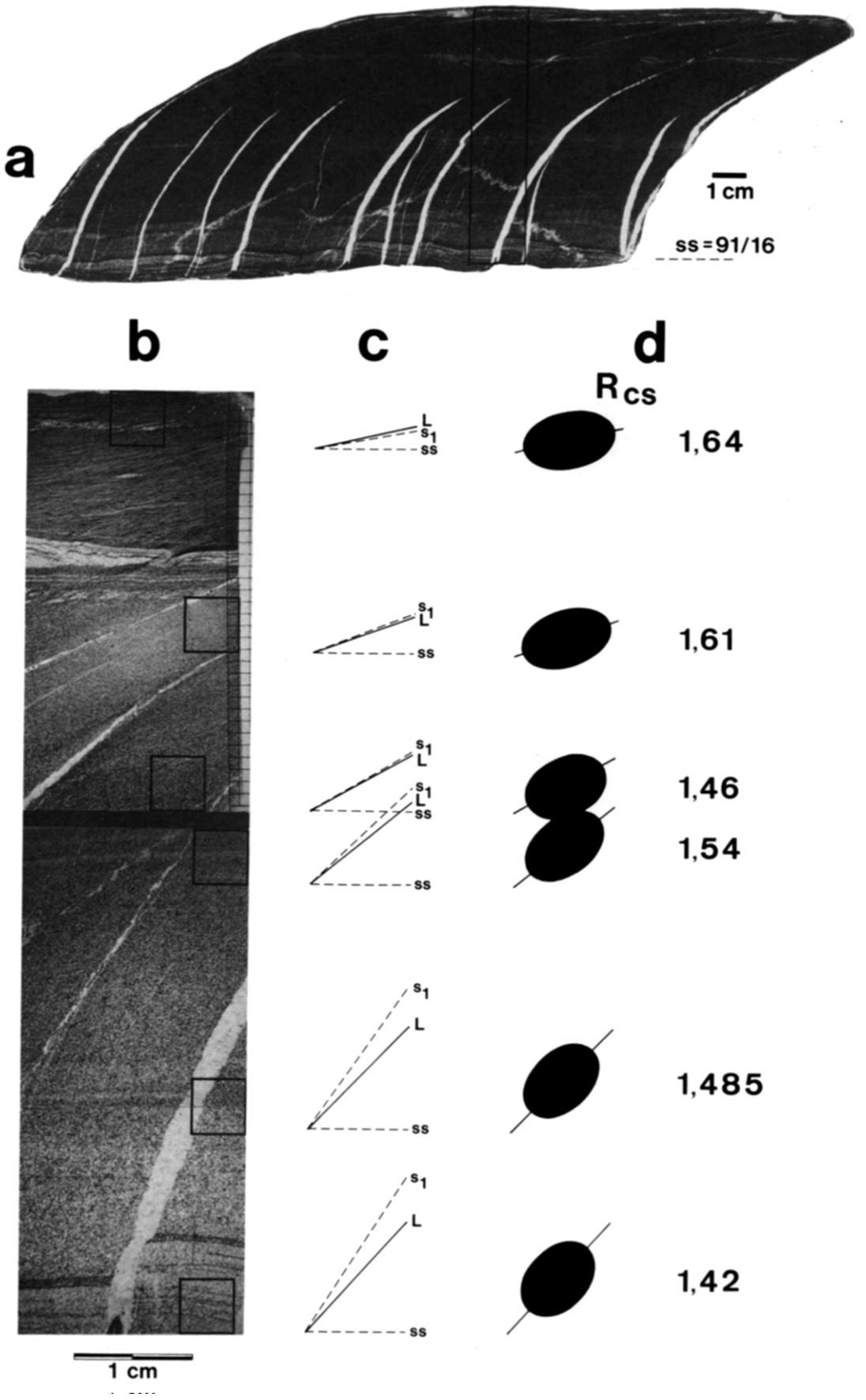

Fig. 5. Finite strain in cross-section (perpendicular to fold axis) through graded bed (a, detail in b) with grain size decreasing from 250 μm at the base to 20 μm at the top and a concomitant continuous cleavage refraction. Traces of bedding (ss), cleavage (s_1) and major ellipse axes (L) are included (c) along with the values of the axial ratios (R_{cs}) of the strain ellipses in the cross-section plane (d). Sample collected from relatively low grade rocks of the Hunsrück nappe.

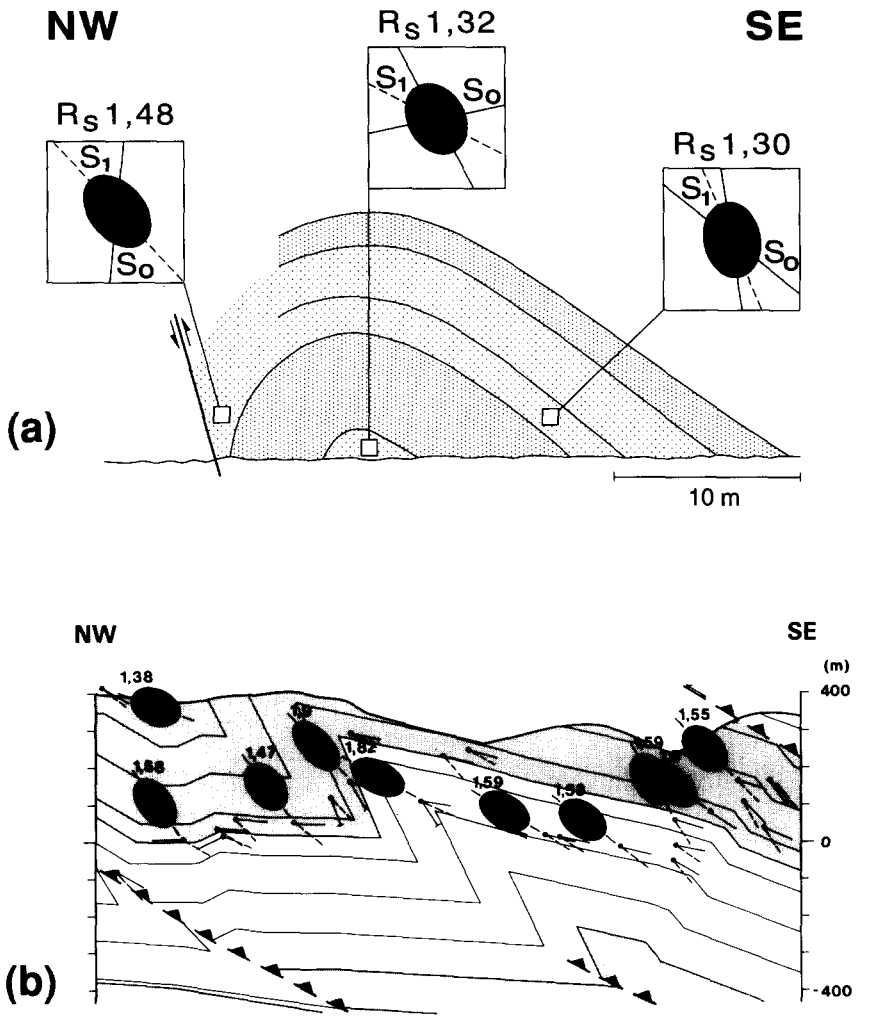

Fig. 6. Finite strain in cross-section plane (R_{cs}) in fault-related folds from (a) unmetamorphic immature sandstones of the northern Massif (with peak strain immediately near reverse fault on steep northwest limb) and (b) a very low grade sequence of sandy shales (stippled) and a quartzite-rich sequence (white) of the Hunsrück nappe. Both diagrams include the traces of bedding (S_0, uninterrupted lines), of principal cleavage (S_1, dashed lines) and of the long ellipse axis (without abbreviation).

assumed—with a general trend to an apparent plane strain geometry (see Fig. 10). The different 'homogeneously' deformed units (see above and Fig. 4) may show specific geometries.

The foreland near the orogenic front and the Eifel Depression show flattening, with a strong component of uniaxial shortening perpendicular to bedding. Compactional strain in these high-level sequences has not been overprinted significantly by deformation although shortening is obvious from folding and minor imbrication (with, however, mostly parallel folds formed by flexural-slip). Weber (1976) made similar observations in the northern Massif based on sheetsilicate fabrics and their orientation with respect to bedding.

Further to the north and the south of the Eifel Depression, the long and intermediate ellipsoid axes can be seen to roughly outline the cleavage plane. The degree of deviation of the axes from the cleavage plane decreases with the increase of strain (Fig. 5). Weakly strained samples still have a memory of compactional strain so that strain axes may lie at oblique angles to bedding as well as to cleavage. Strain geometry in these cases tends to be prolate with the long axis parallel to the fold axes. This effect is a result of the superposition of two obliquely oriented deformation increments (compactional and tectonic) with a concomitant change of the strain geometry from initially oblate (due to compaction) to an early deformational prolate state. This may again evolve to a late deformational plane strain or even oblate geometry (see Ramsay & Wood 1973).

Most regions are characterized by samples which have been deformed at near apparent plane strain geometry (Fig. 10). Both Phyllite Zones (southern Venn and southern Hunsrück) depart from this picture showing predominantly prolate (Venn) or oblate strains (Hunsrück), respectively. The orientation of the strain ellipsoid either shows an approximately downdip orientation of the ellipsoid's long axis within the cleavage plane (northern and central Massif) or an orientation which rather shows an E–W- to NE–SW-trending, oblique to subhorizontal long axis (Hunsrück nappe, Phyllite Zone; Fig. 3b). Although the regional pattern is complicated, this latter orientation is more prominent in the southern Massif. Generally, no clear relationship between orientation of axes, ellipsoid shape, and structural position of the samples can be established at present.

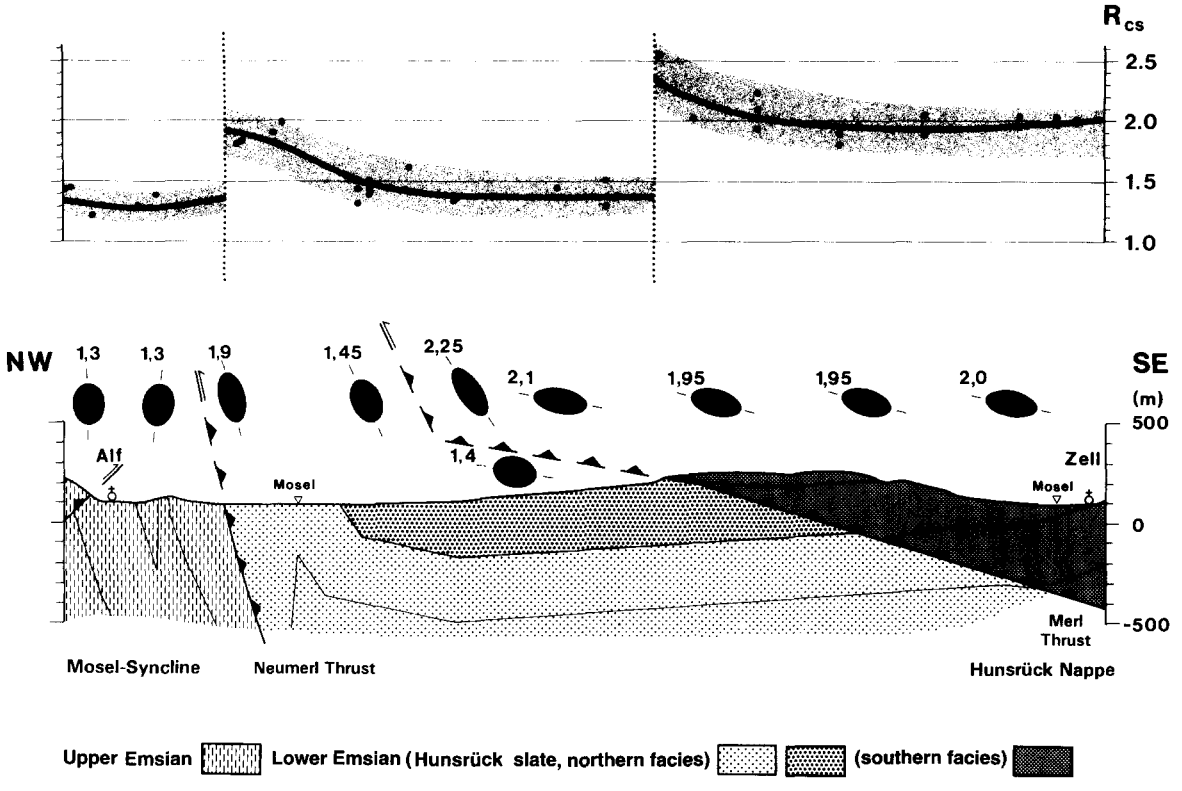

Fig. 7. Finite strain in cross-section (R_{cs}) through a slate-dominated imbricate stack (Boppard–Merl thrust system at front of Hunsrück nappe, see Fig. 3) shoeing average shapes, orientations and axial ratios of strain ellipse. Upper half of figure includes axial ratios of all measurements in a strain–distance diagram; thick black line shows average.

Incremental strain analysis

Although not a principal aim of this study, some incremental strain data have been collected and compiled from other sources in order to evaluate the orientation pattern of the finite strain ellipsoids in relation to the kinematic pattern of the Rhenish Massif. Data are obtained from pressure fringes around pyrite grains and from veins (see Durney & Ramsay 1973 for method).

Face-controlled as well as displacement-controlled growth of syntaxial quartz occurs around pyrite grains. As a rule, analysis is based on the rigid fibre model which appears justified by weak to absent crystal-plastic deformation of the fringes. In several cases it seems that pyrite growth is not preorogenic and the stretching path thus does not always reflect the entire incremental history. Each stretching path on the map (Fig. 11) is averaged from between 2 and 10 pressure shadows within one thin section.

Synkinematic vein generations, on the other hand, appear to occur preferentially during the early and principal stages of deformation, probably due to concentrated hydraulic overpressures during these stages. Growth types mainly include quartz veins, and some calcite veins in carbonates, with a syntaxial to crack–seal fibre geometry at high angles to the vein walls.

Because of the application of different methods and the compilation from different sources, displacement paths on the map in Fig. 11 do not show measured finite lengths but are normalized to a standard length.

The results of incremental strain analysis throw more light on the above observation of complex orientation patterns. The finite stretching axes of pressure shadows for different parts of the Massif show a clear trend: finite stretching at the frontal part of the thrust belt is subperpendicular (NW–SE) to the trend of folds, thrusts and the orogenic front; towards the south this pattern gradually changes to an oblique, E–W-directed finite stretching which, at the southern border of the Massif, may grade into an orogen-parallel stretching (SW–NE). Throughout the Massif only the early incremental strains are subperpendicular to the trend of folds and thrusts.

The orientation of incremental strains merely contains information on the orientation of extension near or within the *XY*-plane, i.e. the cleavage plane, of the rock and has no bearing on an eventual transport direction. Here however, it is interpreted to represent displacement directions for two reasons. The samples were mostly collected immediately above major thrusts; the analysis of indicators of sense of shear at these thrust boundaries in the southern Massif shows that thrust emplacement changed from NW-directed to a late W-directed stage (Oncken 1989). This kinematic pattern is reflected in the oblique orientation patterns of finite strains.

DISCUSSION

Shortening and volume loss in the Rhenohercynian basin

The strain values can be used to calculate the longitudinal shortening of bed-length due to orogenic defor-

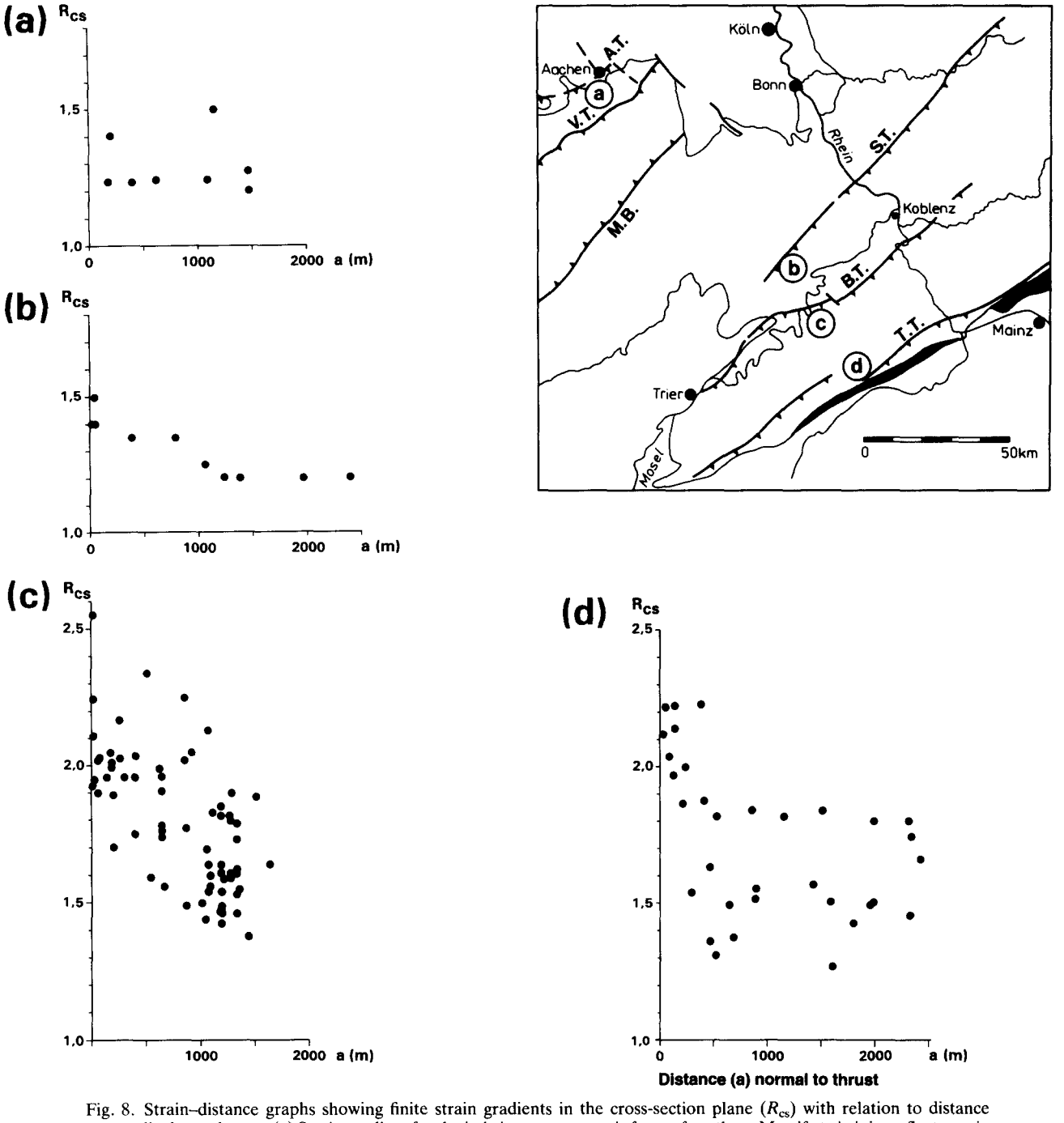

Fig. 8. Strain–distance graphs showing finite strain gradients in the cross-section plane (R_{cs}) with relation to distance perpendicular to thrusts. (a) Strain gradient for the imbricates at orogenic front of northern Massif at vitrinite reflectance in general below 3% R_{max} (Inde syncline south of the Aachen thrust). (b) Strain gradient for imbricates of central Massif with organic rank between 3 and 6% R_{max} (Siegen thrust stack). (c) & (d) Strain gradients for imbricates of southern Massif (Hunsrück nappe, Fig. 3) with organic rank between 5 and 7% R_{max}; (c) from internally unfolded imbricate at front of stack (Fig. 6), (d) from group of internally folded imbricates at rear of stack.

mation (see von Winterfeld 1994 and von Winterfeld & Oncken in preparation for mathematics). The first approach assumes no volumetric change during deformation ($dV = 0$). The regional pattern of bed-length changes is complex in the section plane, i.e. in the NW–SE direction (Fig. 12a): some shortening between −5 and −10% is seen in the northern and in the southern Massif; the central Massif exhibits insignificant changes of length between −4 and 11%. In the southern Venn Anticlinorium, the Siegen thrust stack, and in the southernmost Rhenish Massif bed-length has been stretched by 18, 5–12 and 7–14%, respectively. This is clearly due to the locally small angle between bedding and the trace of the XY- plane of the strain ellipsoid in profile section. The traces of bedding fall within the sector of positive longitudinal strain of the finite strain ellipsoid. Overall deformation of the basin filling (i.e. its original line length) by internal deformation, thus disregarding the effects of imbricate stacking and folding, is almost negligible: the average amounts to 1.5% (=weak stretching).

Stretching of bed length along strike (Fig. 12b) under the same conditions mentioned above in the northern and central Massif ranges between slight shortening

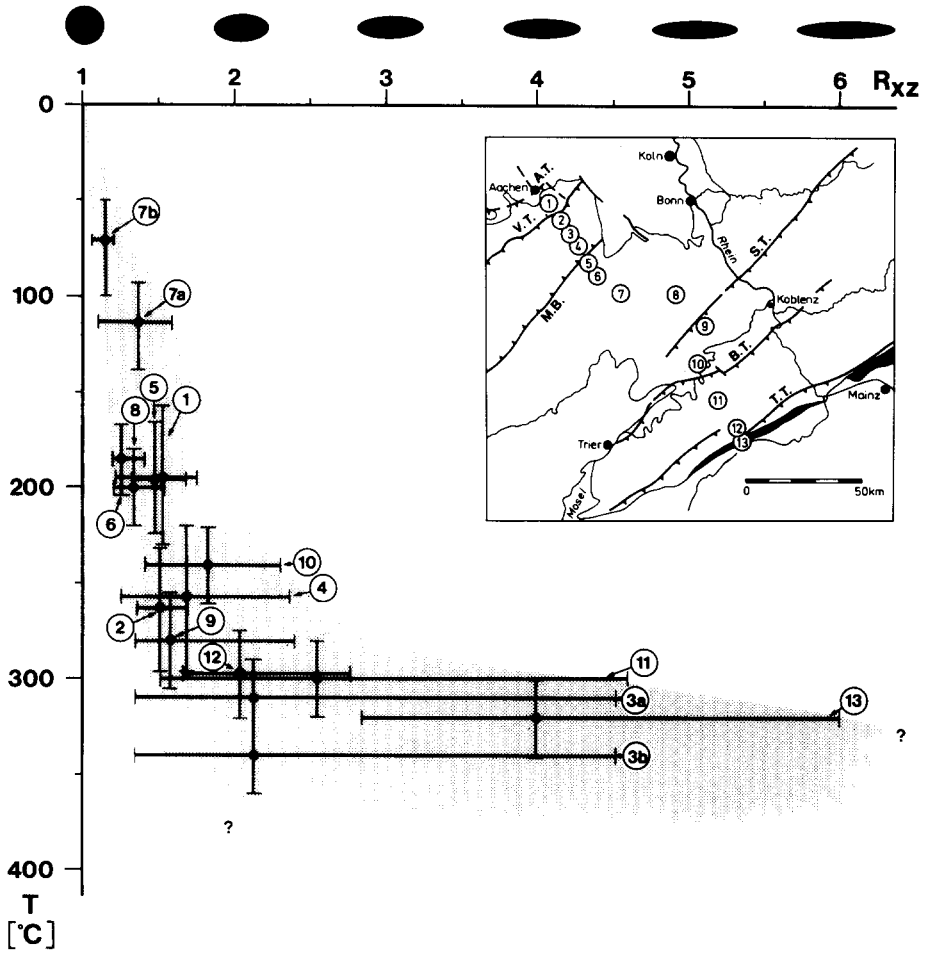

Fig. 9. Strain–temperature graph showing relationship between finite strain in the *XZ*-plane and peak metamorphic temperatures, estimate from vitrinite reflectance, fluid inclusion and petrologic data, for several indicated areas across the entire Massif. Vertical bars show uncertainty in temperature determination, horizontal bars indicate scatter of data. A.T., Aachen thrust; V.T., Venn thrust; M.B., Malsbenden backthrust; S.T., Siegen thrust; B.T., Boppard thrust; T.T., Taunus thrust.

(−8%) to some stretching (25%). In the southern Massif apparent stretching exceeds 25% and may reach 70%. These orogen-parallel extensions appear unrealistically high and call for explanation.

Although the quantitative volumetric part of the total strain has been ignored to this point in the analysis some discussion is warranted. Data of Plessmann (1966) suggest a major volume loss during cleavage formation in parts of the Rhenish Massif (cf. also Breddin 1956, Wunderlich 1964, and equivalent data for other slate belts, Ramsay & Wood 1973, Wood 1974, Wright & Platt 1982, Wright & Henderson 1992). Wintsch *et al.* (1991) however point out that cleavage formation does not necessarily lead to bulk volume loss because redistribution of matter occurs only on a small scale in an otherwise open system. The ubiquitous presence of mineralized veins containing quartz ± chlorite in siliciclastic sediments and calcite in carbonates, and of pressure shadows around competent grains in the Rhenish Massif rocks seems to lend some support to the idea of small, mm- to m-scale redistribution.

Some semi-quantitative considerations however lead to other conclusions. In an earlier study Wood (1974) pointed out that two explanations are generally put forward to account for parallelism of fold axes and ellipsoid long axes: either no volume loss has occurred (resulting in significant elongation along strike; e.g. Cloos 1947), or no true stretching along strike has occurred (which necessitates considerable volume loss to arrive at the observed geometrical relationship; Sorby 1908, Ramsay & Wood 1973, Wood 1974, Beutner & Charles 1985).

The first approach has been discussed above. The second solution would exclude orogen-parallel extension by accounting for the observed deformation pattern by volume loss during deformation of an oblate bedding-parallel compactional ellipsoid. In this case bed-length in cross-section is changed during deformation by an average of some −5% in the north to −14% in the south. The greenschist area of the southern Venn Anticlinorium shows stretching of merely 5 to 8% whereas the Hunsrück Phyllite Zone exhibits up to 38% shortening under these conditions. The corresponding values for volume loss are on average 30–40% near the orogenic front reaching 50–70% with a maximum of 84% at the southern margin of the orogenic wedge.

The case of the Rhenish Massif is believed to lie in between both end-member scenarios. The nearly cylindrical geometry of major structures with an usually more than km-scale continuity does not bear out stretching of

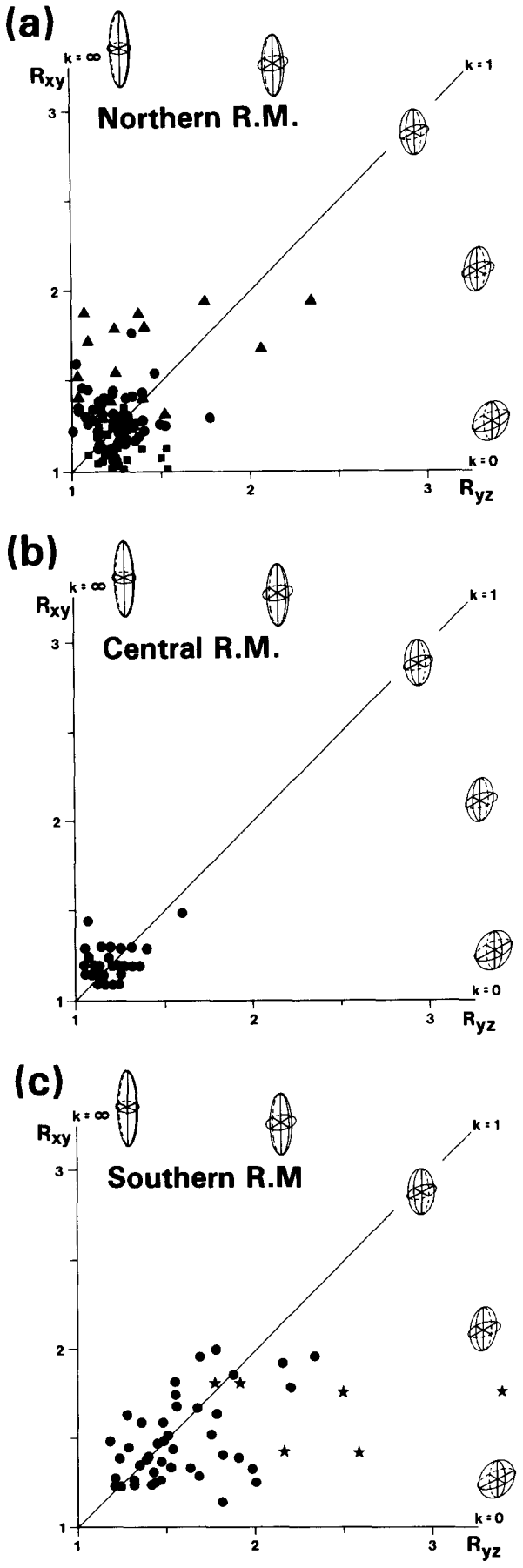

Fig. 10. Flinn diagrams for finite strain geometry of the Northern (a), central (b) and southern (c) Rhenish Massif. Triangles—greenschist facies rocks of southern Venn anticlinorium; squares—Eifel Depression; stars—southern Phyllite Zone. Filled circles include all other regions.

the thrust belt along strike by as much as 70%. On the other hand, veining subperpendicular to fold axes, axial culminations and depressions, and steeply dipping late wrench faults indicate minor stretching of the belt along strike. Moreover, a few data on volumetric strain collected by von Winterfeld (1994) in the northern Massif suggest small scale volume losses in the order of 15–50% depending on lithology and metamorphic grade. This is well in the range usually cited for slate belts (e.g. Sorby 1908, Breddin 1957, Plessmann 1966, Ramsay & Wood 1973, Wood 1974, Wright & Platt 1982, Beutner & Charles 1985, Wright & Henderson 1992).

Considering these values, the first named numbers for layer-parallel shortening in cross-section (see Fig. 12a) roughly increase by up to 50%. The same volume losses reduce the above strike-parallel stretching values to zero in the north and to a now smaller amount of less than 10–25% in the south. The arcuate geometry of the Ardennes and the western continuation of the southern Rhenish Massif can account for increasing along-strike stretching towards the south and west reaching up to 15% due to bending of the thrust wedge above a vertical axis. Larger values will lead to severe strain compatibility problems along the strike of the orogen. Possibly, this argument is a further clue to the amount of material and porosity lost during deformation in the southern Massif.

On the whole, the finite strains measured considerably underestimate changes of bed-length, basin width and crustal shortening when disregarding volume losses. It needs to be mentioned, however, that deduction of volumetric data from the orientation and geometry of finite strains is rendered more ambiguous by an important aspect. Incremental strain data point towards a more complex collisional history (see below) which suggests several stages which were not coaxial. True orogen-parallel stretching may thus have overprinted the sequence of compactional strain and the subsequent tectonic strain perpendicular to the belt.

Net orogenic shortening of the Rhenohercynian upper crust of approximately 42% is mainly achieved by tectonic stacking, i.e. 'brittle' strain of the deformed basin filling. The contribution of distributed ductile deformation in imbricates, as recorded in the finite strain data, to overall horizontal shortening reaches values between 0% (orogenic front) and a maximum of 51% at the southern rim of the Massif assuming no volume loss. If volume loss is important the contribution of shortening by internal deformation with respect to earth coordinates (i.e. the horizontal) is still larger. Changes of bed length (i.e. shortening with respect to internal co-ordinates parallel to bedding), on the other hand, are small (see above values).

Partitioning of deformation and displacement in the orogenic wedge

Diffuse contraction of the former passive continental margin upon collision with the Saxothuringian zone shows partitioning of deformation at a variety of scales.

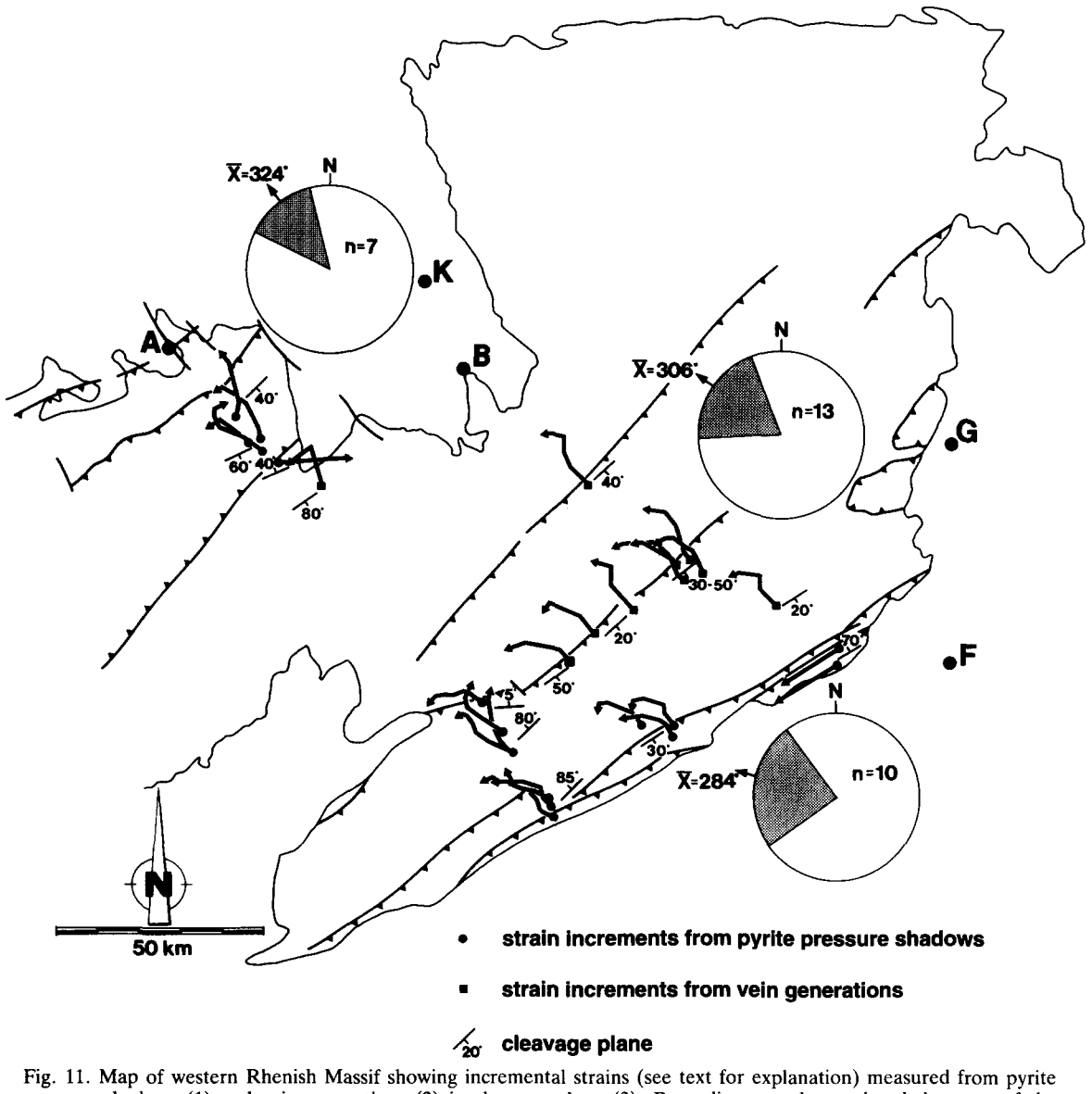

Fig. 11. Map of western Rhenish Massif showing incremental strains (see text for explanation) measured from pyrite pressure shadows (1) and vein generations (2) in cleavage plane (3). Rose diagrams show azimuthal scatter of the orientation of the finite stretching vectors for northern Massif, southern Massif, and southern rim of the Rhenish Massif. Arrows give arithmetic mean of measured directions. Data are compiled from Oncken (1989), Elbert (1990), von Winterfeld (1993) and include new data. Length of arrows is normalized to a standard length which only gives percentage of increments.

On the hand specimen and outcrop scale, the influence of grain size distribution or minor structures (folds) dominates. On the quadrangle map-scale thrusts control the distribution of deformation with increasing strain towards the base of hangingwalls. Thrusts moreover ensure the compatibility of strain across the observed discontinuous changes of finite strain from hangingwalls to footwalls. The orogen-wide strain pattern is related to varying metamorphic grades (i.e. temperatures). The superposition of these parameters with their different wavelengths and with the repetition of strain gradients at different scales suggests a self-similar geometry.

The amount of deformation is loosely tied to the former structural depth of the sampled rocks in the orogenic wedge; an increase with rising temperatures, i.e. with depth, is obvious. At high crustal levels deformation is strongly localized in a network of discrete faults. The deformation is progressively delocalized with the onset of thermally activated, especially grain-size sensitive and lithology-controlled deformation mechanisms.

Although deformation probably started during prograde conditions and outlasted peak metamorphic conditions, most of the finite strain was accumulated during the thermal peak. This is corroborated by the relation of the timing of fabric formation to peak thermal conditions: The finite strain ellipsoids are closely related to the dominant pervasive cleavage; the latter was largely formed at peak thermal conditions during maximum burial (Weber 1976, Ahrendt *et al.* 1983, Oncken 1991). The above relationship thus records deformation conditions at the former structural level in the orogenic wedge.

The T-dependent strain pattern also reflects the change of the flow pattern of the upper crust across the so called brittle zone during orogenic contraction.

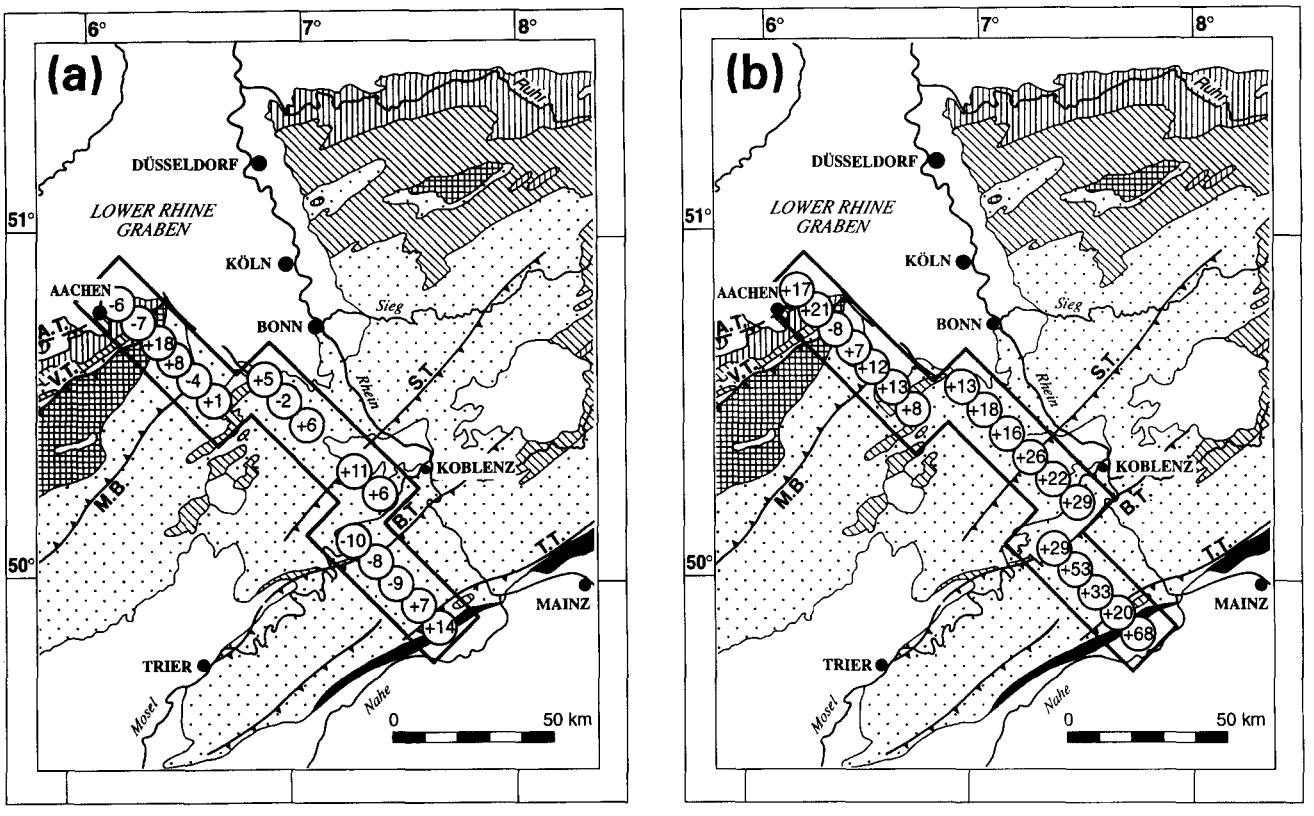

Fig. 12. Changes of bed length in the western Rhenish Massif (constant volume assumed) during deformation perpendicular to strike (a) and along strike (b) averaged for several 'homogeneously' deformed units and solely related to bedding co-ordinates (not to earth or to strain co-ordinates!). Positive numbers show stretching, negative numbers correspond to shortening. A.T., Aachen thrust; V.T., Venn thrust; M.B., Malsbenden backthrust; S.T., Siegen thrust; B.T., Boppard thrust; T.T., Taunus thrust.

Although the simple rheological zonation of the crust has been repeatedly criticized on the basis of empirical data or of arguments invoking the complexities of nature, the above notion still forms a much used powerful theoretical framework for infering the internal structure and strength of a rheologically layered crust. The response to shortening in the case presented supports the notion that deformation is increasingly pervasive with increasing temperatures and depths showing a broad zone with transitional behaviour which links the uppermost with the middle crust. Narrow zones of concentrated deformation persist through the entire pile analysed while the enclosed thrust units develop a specific shear zone related strain pattern with increasing temperatures.

The latter aspect and the elevated strains in overturned limbs of still coherent fault-propagation folds (see Fig. 6b) suggest a further relationship: a ductile bead may have passed ahead of most evolving shear zones (cf. Elliott 1976, Williams & Chapman 1983) (cf. also Fig. 6b) with probably also some distributed simple shear at the base of the sheets during the early stage of thrusting. Subsequent deformation appears to have concentrated into more narrowly confined zones, controlled either by mechanisms of strain localization in existing faults (see White *et al.* 1986, Oncken 1989) or/and by increasing embrittlement during exhumation and cooling of the thrust stack.

However, the relationship between a given strain pattern and the former structural–metamorphic situation is not simple. Field and fabric relationships (cataclastic overprinting of mylonites and of foliated cataclasites, juxtaposition of rocks with different metamorphic grade at thrusts, cleavage generations with different fabric forming processes) clearly indicate that part of the deformation proceeds under changing conditions (i.e. decreasing temperatures, effective confining pressures, etc.) and causes the formation of out-of-sequence structures. In particular, the superposition of non-coaxial increments during progressive deformation may obscure any simple relationship.

This is seen in the related internal kinematics of the thrust wedge which evolved through several stages of non-homoaxial deformation increments as shown from the analysis of pressure shadows and veins. Similarly, the analysis of kinematic axes from faults and striae (Oncken 1988) yields an anticlockwise rotation of the principal direction of shortening especially in the southern Massif and less pronounced in the northern Massif. Parts of the Eifel Nappe bear some indications to an earlier clockwise rotation of the shortening direction. These changes of shortening direction must have been the result of one or both of two scenarios: Lower Carboniferous pre- to syncollisional head on convergence at the continental boundary may have been followed by a switch to postcollisional dextral transpression during Upper Carboniferous times, or convergence of the Saxothuringian microplate was oblique throughout.

In the latter case, the kinematics of the thrust bodies should have been governed by their respective position in the orogenic wedge: at the tip of the wedge thrusting was foreland-directed, perhaps strongly influenced by body forces at the front of a foreland-propagating, critically tapered wedge. As the imbricates were progressively incorporated in the internal or rear parts of the wedge during its growth by foreland accretion, the dextral motion of the upper plate was increasingly 'felt' with a concomittant out-of-sequence displacement of the imbricates to the west.

Cashman *et al.* (1992) have described similar patterns of strain partitioning between different structural domains, equivalent to thrust-bounded units in the present study, at the active plate margin in New Zealand which exhibits strongly oblique convergence. Heterogeneities of incremental strain distribution and of orientation of finite strain and kinematic axes thus most probably record deformation partitioning due to oblique plate convergence of the Rhenohercynian–Saxothuringian plates.

CONCLUSIONS

From the above analysis several conclusions may be drawn regarding the geometry of deformation of foreland fold and thrust belts in general and the Rhenish Massif in particular.

—Volumetric strain and orogen-parallel stretching still pose fundamental problems barely understood. Systematical studies are lacking.

—Strain geometry in slate belts may vary to a larger degree than generally assumed. Finite stretching geometries in pelites clearly are possible depending on the mode of superposition of non-homoaxial incremental strains.

—Construction of balanced sections without incorporating three-dimensional strain data may lead to badly constrained solutions. Area is nowhere conserved in the Rhenish Massif with its rather simple internal geometry. Changes of cross-sectional area and also out of section displacement both have to be corrected for.

—The axial ratios measured, between 1 and 6 in the XZ-plane with an average around 2, are identical to those encountered under similar conditions of lithology, metamorphic grade, etc. in similar orogenic belts (compare data compilation in Pfiffner & Ramsay 1982). Taking into account the orientation of strain axes with respect to bedding, these values correspond to a surprisingly weak general layer-parallel shortening of the basin filling in cross-section on the order of about 5–15% and more in the case of volume loss. Net orogenic shortening in the upper crust of the fold and thrust belt is approximately 42%. It is mainly achieved by folding and tectonic stacking of the deformed basin filling, which was apparently detached from the lower crust.

—The orientation of the strain ellipsoid shows complex patterns: from compactional strains perpendicular to bedding in unmetamorphic areas, to reorientation of the ellipsoid parallel to fold axes, and, at still larger strains and very low–low grade conditions, rotation of the ellipsoid into the evolving cleavage plane with no systematical orientation across the Massif (a relationship to stretching lineations may exist, none however is observed with respect to fold axes at higher strains).

—Heterogeneous strain is caused by changes in lithology and average grain size, by the structural position of samples in folds and their distance from thrusts in the hangingwall (at deeper crustal levels). The superposition of these strain partitioning mechanisms on different scales creates a complex regional strain pattern in terms of magnitude and orientation.

—An important crustal-scale strain partitioning mechanism is the regional distribution of metamorphic grade which exerts major control over the dominant deformation mechanism. The increasing importance of thermally activated deformation mechanisms causes an exponential increase of finite strain including increasing variability with approach to the ductile lower crust across a broad transitional zone. No discrete brittle-ductile transition is observed.

—The southern part of the thrust belt apparently suffered late westward motion (in gently dipping imbricates) or strike-parallel dextral motion (in steeply dipping imbricates) which is probably due to oblique convergence between the Rhenohercynian and Saxothuringian microplates.

Acknowledgements—The present study has been generously funded by the Deutsche Forschungsgemeinschaft (No. Wa 365/13-1-4) which is gratefully acknowledged. The paper has greatly profited from discussions with many colleagues, especially from fruitful criticisms on earlier versions of the manuscript by P. Bankwitz, J. Behrmann and G. Dresen. Constructive and detailed reviews by J. Henderson, C. W. Passchier and K. Weber finally have helped to find the present form of the paper.

REFERENCES

Ahrendt, H., Clauer, N., Hunziker, J.C. & Weber, K. 1983. Migration of folding and metamorphism in the Rheinisches Schiefergebirge deduced from K–Ar and Rb–Sr age determinations. In: *Intracontinental Fold Belts. Case Studies in the Variscan Belt of Europe and the Damara Belt in Namibia* (edited by Martin, H. & Eder, F. W.). Springer, Berlin, 323–338.

Anderle, H.-J., Massonne, H.-J., Meisl, S., Oncken, O. & Weber, K. 1990. Southern Taunus Mountains. In: *Field Guide to Mid German Crystalline Rise and Rheinisches Schiefergebirge (Int. Conf. on Paleozoic Orogens in Central Europe)*, Göttingen-Gießen 1990, 125–148.

Behrmann, J., Drozdzewski, G., Heinrichs, T., Huch, M., Meyer, W. & Oncken, O. 1991. Crustal-scale balanced cross sections through the variscan fold belt, Germany: the central EGT-segment. *Tectonophysics* **196**, 1–21.

Beutner, E. C. & Charles, E. G. 1985. Large volume loss during cleavage formation, Hamburg sequence, Pennsylvania. *Geology* **13**, 803–805.

Breddin, H. 1956. Die tektonische Deformation der Fossilien im Rheinischen Schiefergebirge. *Z. dt. geol. Ges.* **106**, 227–305.

Breddin, H. 1957. Tektonische Fossil- und Gesteinsdeformation im Gebiet von St. Goarshausen (Rheinisches Schiefergebirge). *Decheniana* **110**, 289–350.

Cashman, S., Kelsey, H. M., Erdman, C. F., Cutten, H. N. C. & Berryman, K. R. 1992. Strain partitioning between structural domains in the forearc of the Hikurangi subduction zone, New Zealand. *Tectonics* **11**, 242–257.

Cloos, H. 1947. Oolite deformation in the South Mountain Fold, Maryland. *Bull. geol. Soc. Am.* **58**, 843–918.

DEKORP Research Group. 1985. First results and preliminary interpretation of deep-reflection seismic recordings along profile DEKORP 2-South. *J. geophys.* **57**, 137–165.

DEKORP Research Group. 1991. Results of the DEKORP 1 (BELCORP-DEKORP) deep seismic reflection studies in the western part of the Rhenish Massif. *Geophys. J. Int.* **106**, 203–227.

De Paor, D. G. 1988. R_f/ϕ_f strain analysis using an orientation net. *J. Struct. Geol.* **10**, 323–333.

Dietrich, D. 1989. Fold-axis parallel extension in an arcuate fold- and thrust belt: the case of the Helvetic nappes. *Tectonophysics* **170**, 183–212.

Dittmar, U. 1994. Deformation und Profilbilanzierung durch das linksrheinische südliche Schiefergebirge (Hunsrück). Unpublished Ph.D. thesis, Würzburg.

Dittmar, U. & Oncken, O. 1992. Anatomie und Kinematik eines passiven varistischen Kontinentalrandes—zum Strukturbau des südwestlichen Rheinischen Schiefergebirges. *Frankf. geowiss. Arb.* **A11**, 34–37.

Dunne, W. M., Onash, C. M. & Williams, R. T. 1990. The problem of strain marker centers and the Fry-method. *J. Struct. Geol.* **12**, 933–938.

Dunnett, D. 1969. A technique of finite strain analysis using elliptical particles. *Tectonophysics* **7**, 117–136.

Durney, D. W. & Ramsay, J. G. 1973. Incremental strains measured by syntectonic crystal growth. In: *Gravity and Tectonics* (edited by De Jong, K. A. & Schloten, R.). Wiley, New York, 67–96.

Eisbacher, G. H., Lüschen, E. & Wickert, W. 1989. Crustal-scale thrusting and extension in the Hercynian Schwarzwald and Vosges, Central Europe. *Tectonics* **8**, 1–21.

Elbert, W. 1990. Geologische Untersuchungen im Bereich der Bopparder Überschiebungszone – Rheinisches Schiefergebirge (TK 5612 Bad Ems und TK 5712 Dachsenhausen). Unpublished thesis, Frankfurt.

Elliott, D. 1976. The motion of thrust sheets. *J. geophys. Res.* **81**, 949–963.

Engel, W. & Franke, W. 1983. Flysch sedimentation: its relations to tectonism in the European Variscides. In: *Intracontinental Fold Belts. Case Studies in the Variscan Belt of Europe and the Damara Belt in Namibia*. Springer, Berlin, 289–321.

Engel, W., Franke, W., Grote, C., Weber, K., Ahrendt, H. & Eder, F. W. 1983. Nappe tectonics in the southeastern part of the Rheinisches Schiefergebirge. In: *Intracontinental Fold Belts. Case Studies in the Variscan Belt of Europe and the Damara Belt in Namibia* (edited by Martin, H. & Eder, F. W.). Springer, Berlin, 267–287.

Engelder, T. 1984. The role of porewater circulation during the deformation of foreland fold and thrust sheets. *J. geophys. Res.* **89**, 4319–4325.

Erslev, E. A. 1988. Normalised centre-to-centre strain analysis of packed aggregates. *J. Struct. Geol.* **10**, 201–209.

Erslev, E. A. & Ge, H. 1990. Least-squares centre-to-centre and mean object ellipse fabric analysis. *J. Struct. Geol.* **12**, 1047–1059.

Franke, W. 1989. Tectonostratigraphic units in the Variscan belt of central Europe. *Spec. Pap. geol. Soc. Am.* **230**, 67–90.

Franke, W., Bortfeld, R. K., Brix, M., Drozdzewski, G., Dürbaum, H. J., Giese, P., Janoth, W., Jödicke, H., Reichert, C., Scherp A., Schmoll, J., Thomas, R., Thünker, M., Weber, K., Wiesner, M. G. & Wong, H. K. 1990. Crustal structure of the Rhenish Massif: Results of deep seismic reflection lines DEKORP 2 North and 2 North-Q. *Geol. Rdsch.* **79**, 523–566.

Frisch, W., Neubauer, F. & Satir, M. 1984. Concepts of the evolution of the Austroalpine basement complex (Eastern Alps) during the Caledonian–Variscan cycle. *Geol. Rdsch.* **73**, 47–68.

Fry, N. 1979. Random point distributions and strain measurement in rocks. *Tectonophysics* **60**, 89–105.

Groshong, R. H. Jr. 1975. Strain, fractures, and pressure solution in natural single layer folds. *Bull. geol. Soc. Am.* **86**, 1363–1376.

Grösser J. & Dörr, W. 1986. MOR-Typ-Basalte im östlichen Rheinischen Schiefergebirge. *Neues Jb. Geol. Paläont. Mh.* **12**, 705–712.

Korsch, G. & Schäfer, A. 1991. Geological interpretation of DEKORP deep seismic reflection profiles 1C and 9N across the Variscan Saar Nahe Basin, southern Germany. *Tectonophysics* **191**, 127–146.

Kossmat, F. 1927. Gliederung des varistischen Gebirgsbaus. *Abh. Sächs. geol.* L.-A. **1**, 1–39.

Langheinrich, G. 1976. Verformungsanalyse im Rhenoherzynikum. *Geotekt. Forsch.* **51**.

Lisle, R. J. 1977. Estimation of the tectonic strain ratio from the mean shape of the deformed elliptical markers. *Geol. Mijnb.* **56**, 140–144.

Lorenz, V. & Nicholls, I. A. 1984. Plate and intraplate processes of Hercynian Europe during the Late Paleozoic. *Tectonophysics* **107**, 25–56.

Matte, Ph. 1986. Tectonics and plate tectonics model for the Variscan belt of Europe. *Tectonophysics* **126**, 329–374.

Meisl, S. 1990. Metavolcanic rocks in the "Northern Phyllite Zone" at the southern margin of the Rhenohercynian Belt. In: *Field Guide to "Mid German Crystalline Rise and Rheinisches Schiefergebirge" (Int. Conf. on Paleozoic Orogens in Central Europe)*, Göttingen–Gießen 1990, 25–42.

Meyer, W. & Stets, J. 1980. Zur Paläogeographie von Unter- und Mitteldevon im westlichen und zentralen Rheinischen Schiefergebirge. *Z. dt. geol. Ges.* **131**, 725–751.

Oncken, O. 1988. Aspects of the reconstruction of the paleo-stress-history of a fold and thrust belt (Rhenish Massif, Federal Republic of Germany). *Tectonophysics* **152**, 19–40.

Oncken, O. 1989. Geometrie, Deformationsmechanismen und Paläospannungsgeschichte großer Bewegungszonen in der höheren Kruste (Rheinisches Schiefergebirge). *Geotekt. Forsch.* **73**, 1–215.

Oncken, O. 1991. Aspects of the structural and paleogeothermal evolution of the Rhenish Massif. *Ann. Soc. Géol. Belg.* **113**, 139–159.

Pfiffner, O. A. 1980. Strain analysis in folds (Infrahelvetic complex, Central Alps). *Tectonophysics* **61**, 337–362.

Pfiffner, O. A. & Ramsay, J. G. 1982. Constraints on geological strain rates: arguments from finite strain states of naturally deformed rocks. *J. geophys. Res.* **87**, 311–321.

Paterson, S. R. 1983. A comparison of methods used in measuring finite strains from ellipsoidal objects. *J. Struct. Geol.* **5**, 611–618.

Plessmann, W. 1966. Lösung, Verformung, Transport und Gefüge (Beiträge zur Gesteinsverformung im nordöstlichen Rheinischen Schiefergebirge). *Z. dt. geol. Ges.* **115**, 650–663.

Ramsay, J. 1967. *Folding and Fracturing of Rocks*. McGraw Hill, New York.

Ramsay, J. & Wood, D. S. 1973. The geometric effects of volume change during deformation processes. *Tectonophysics* **16**, 263–277.

Ramsay, J. & Huber, M. 1983. *Modern Techniques of Structural Geology, Vol. 1. Strain analysis*. Academic Press, London.

Ratschbacher, L. 1987. Quantification of deformation: Evaluation and comparison of strain-analysis techniques in metaconglomerates and phyllites of the Veitsch Nappe (Eastern Alps). *Neues Jb. Geol. Paläont. Mh.* **1987**, 332–352.

Reks, I. J. & Gray, D. R. 1983. Strain patterns and shortening in a folded thrust sheet: an example from the southern Appalachians. *Tectonophysics* **93**, 99–128.

Schievenbusch, T. 1992. Bilanzierte Profile, Profilabwicklung und Verformungsanalyse im westlichen Rheinischen Schiefergebirge zwischen Stötenicher Kalkmulde und Moselmulde. *Bonner Geowiss. Schriften* **3**.

Sorby, H. C. 1908. On the application of quantitative methods to the study of the structure and history of rocks. *Q. J. geol. Soc. Lond.* **64**, 171–232.

Teichmüller, M. & Teichmüller R. 1979. Ein Inkohlungsprofil entlang der linksrheinischen Geotraverse von Schleiden nach Aachen und die Inkohlung in der Nord-Süd-Zone der Eifel. *Fortschr. Geol. Rheinld. Westf.* **27**, 323–355.

Treagus, J. E. & Treagus, S. H. 1981. Folds and the strain ellipsoid: a general model. *J. Struct. Geol.* **3**, 1–17.

Treagus, S. H. 1988. Strain refraction in layered systems. *J. Struct. Geol.* **10**, 517–527.

von Raumer, J. & Neugebauer. F. 1993. Late Precambrian and Paleozoic evolution of Alpine basement—an overview. In: *Pre-Mesozoic Geology in the Alps* (edited by Raumer, J. F. & Neubgeauer, F.). Springer, Berlin, 625–639.

von Winterfeld, C. 1993. Variszische Deckentektonik und devonische Beckengeometrie der Nordeifel – Ein quantitatives Modell (Profilbilanzierung und Strain-Analyse im Linksrheinischen Schiefergebirge. *Aachener Geowiss. Beiträge* **2**.

Weber, K. 1976. Gefügeuntersuchungen an transversal geschieferten Gesteinen aus dem östlichen Rheinischen Schiefergebirge. *Geol. Jb.* **D15**, 3–98.

Weber, K. 1986. The Mid-European Variscides in terms of allochthonous terrains. In: *Proc. 3rd Workshop EGT: The Central Segment* 14–16.4.1986 (edited by Freeman, R., Mueller, S. & Giese, P.). European Science Foundation, 73–82.

Weber, K. & Behr, H. J. 1983. Geodynamic interpretation of the Mid-European Variscides. In: *Intracontinental Fold Belts. Case Studies in the Variscan Belt of Europe and the Damara Belt in Namibia* (edited by Martin, H. & Eder, F. W.). Springer, Berlin, 427–469.

White, S. H., Bretan, P. G. & Rutter, E. H. 1986. Fault-zone reactivation: kinematics and mechanisms. *Phil. Trans. R. Soc. Lond.* **A317**, 81–97.

Williams, G. & Chapman, T. 1983. Strains developed in the hanging-walls of thrusts due to their slip/propagation rate: a dislocation model. *J. Struct. Geol.* **5**, 563–571.

Wintsch, R. P., Kvale, C. M. & Kisch, H. J. 1991. Open-system, constant-volume development of slaty cleavage, and strain-induced replacement reactions in the Martinsburg formation, Lehigh Gap, Pennsylvania. *Bull. geol. Soc. Am.* **103**, 916–927.

Wojtal, S. 1986. Deformation within foreland thrust sheets by populations of minor faults. *J. Struct. Geol.* **8**, 341–360.

Wolf, M. 1978. Inkohlungsuntersuchungen im Hunsrück (Rheinisches Schiefergebirge). *Z. dt. geol. Ges.* **129**, 217–227.

Wood, D. S. 1974. Current views of the development of slaty cleavage. Annu. Rev. *Earth & Planet. Sci.* **2**, 369–401.

Woodward, N. B., Gray, D. R. & Spears, D. B. 1986. Including strain data in balanced cross-sections. *J. Struct. Geol.* **8**, 313–324.

Wright, T. O. & Henderson, J. R. 1992. Volume loss during cleavage formation in the Meguma Group, Nova Scotia, Canada. *J. Struct. Geol.* **14**, 281–290.

Wright, T. O. & Platt, L. B. 1982. Pressure dissolution and cleavage in the Martinsburgh Shale. *Am. J. Sci.* **282**, 122–135.

Wunderlich, H. G. 1964. Maß, Ablauf und Ursachen orogener Einengung am Beispiel des Rheinischen Schiefergebirges, Ruhrkarbons und Harzes. *Geol. Rdsch.* **54**, 561–582.

Ziegler, P. A. 1986. Geodynamic model for the Paleozoic crustal consolidation of Western and Central Europe. *Tectonophysics* **126**, 303–328.